Eduvest – Journal of Universal Studies
Volume 5 Number 7, July, 2025
p- ISSN 2775-3735- e-ISSN 2775-3727

PILE ANALYSIS WITH DYNAMIC AND STATIC TESTS OF MANUFACTURING PERMIT CAPACITY

Dian Kurniawan Tanjung
Universitas Trisakti, Indonesia
*Corresponding Author: diankurniawan.tanjung@outlook.com

DATE

Accepted:
Revised:
Published:

ABSTRACT

This article discusses the analysis of pile bearing capacity using dynamic and static tests to evaluate the capacity of manufacturing permits in the construction project of the X Shoe Factory in Pekalongan, Central Java. The study aims to determine the ultimate bearing capacity of piles by applying various formulas, such as Meyerhoff, Poulos & Davis, Schmertmann, Coyle & Castillo, and the Alpha & Lambda Method, which take into account corrected NSPT values and CPT data. Additionally, the study validates the calculation results through static and dynamic testing, and compares these results with the allowable loads specified in the design and manufacturing management standards. The analysis revealed that the 1956 Meyerhoff method, when combined with the Terzaghi correction for NSPT data, produced results closest to the empirical test values, while the modified ENR formula yielded reliable outcomes for dynamic analysis. This research is expected to enhance efficiency in the selection of appropriate pile foundation systems for future manufacturing facility construction projects.

KEYWORDS *Pile bearing capacity, dynamic test, static test, NSPT, CPT, Meyerhoff, ENR modification.*

INTRODUCTION

In a building, construction consists of elements of the superstructure and the substructure. The substructure comprises the foundation, which is the lowest part of the building in contact with the ground and transfers the load from the building to the soil (Awad et al., 2021; Gernsbacher, 1991; Svatoš-Ražnjević et al., 2022; Zhao, 2024). The foundation is a critical component in construction and can be broadly categorized into shallow foundations and deep foundations. The selection between shallow and deep foundations is influenced by several factors, including site location and load position, physical examination of the geological strata and soil type, results of soil investigation and laboratory test reports, and soil parameters obtained from laboratory test results (Liu et al., 2023; Tang et al., 2024; Zhang et al., 2024).

According to Joseph E. Bowles (1997), shallow foundations are typically used in simple buildings that do not require deep excavation, provided the soil layer is sufficiently strong to support the building loads. For large-scale construction, such as commercial and industrial buildings or infrastructure (e.g., bridges, coastal structures), deep foundations are utilized. Deep foundations are further divided into two types: drilled foundations and pile foundations (Belaroussi et al., 2023; Chen et al., 2023; Khosravani & Haghighi, 2022; Mechtcherine et al., 2019; Puzatova et al., 2022).

It is crucial for practitioners to determine the actual bearing capacity achieved by the constructed foundation to ensure that it can adequately support the building loads transferred through the foundation to the underlying soil strata. In the industrial construction of the X Shoe Factory located in Pekalongan, Central Java, the building consists of two main elements: a steel superstructure and a substructure utilizing pile foundations with *box piles* measuring 250 x 250 mm, with design depths ranging from 6 to 14 meters below the building surface. The soil conditions consist of rocky red soil with hard layers, indicated by Standard Penetration Test (SPT) values above 60 at varying depths. The design bearing capacity is 30 tons per pile, with a safety factor of 200% and a final set acceptance of 250 mm. The design length of the piles for each building varies according to soil conditions, based on soil investigation results, with pile lengths of 6 m, 8 m, 10 m, and 14 m.

During pile installation, the embedded pile lengths varied significantly, with piling terminated once the required drop height was achieved according to the characteristics of the pile driving hammer and the attainment of the final set (Flynn & McCabe, 2019; GENDRON GJ, 1970; Nietiedt et al., 2023; Saher et al., 2024). To estimate the temporary capacity of the piles, the foundation contractor used a pile capacity table based on the dynamic formula *Engineering News Record (ENR) Modification*, determined by the hammer type, drop height, and final settlement value. At the end of the installation, several test samples were taken from installed piles to determine their bearing capacity against the design criteria.

This research has several clear and structured objectives. First, the primary objective is to determine the ultimate bearing capacity of the foundation using various formulas, namely the *Meyerhoff (1956)*, *Poulos & Davis*, *Schmertmann*, *Coyle & Castillo* formulas, and the Alpha & Lambda Method, considering *NSPT* values corrected according to *Terzaghi* and *Skempton*, based on soil stratification data and *CPT* (Cone Penetration Test) values. Second, this study aims to validate the calculated *Qult* values from the aforementioned formulas with static (Mazurkiewicz & Chin) and dynamic (Case Pile Wave Analysis Program [CAPWAP]) test results. Third, validation is also conducted on the *Qult* calculations using the *Hiley* formula and *ENR* modification, compared with the same static and dynamic test results. Furthermore, this study compares the validation results with the permissible design load and the allowable load from manufacturing specifications. Finally, the study aims to assess the cost efficiency of pile foundation implementation, as well as to optimize the depth, length, and dimensions of foundation piles for future use under similar conditions.

In terms of benefits, this study is expected to provide the most reliable static and dynamic formulas for peak bearing capacity, ensuring results that closely match the peak values obtained from static and dynamic pile testing. Additionally, the study aims to identify efficiencies in selecting the appropriate type of pile foundation based on capacity data provided by manufacturing, thereby enhancing effectiveness and efficiency in future construction projects.

METHOD

This research was conducted on the F2 Building construction project at a shoe factory located in *Wangandowo* Village, Pekalongan Regency. The research data utilized consist of primary data collected during the construction process, including variables such as *NSPT* and *CPT* values, pile driving records (*pile driving log*), static load test results, and *CAPWAP* analysis results from dynamic load tests. In addition, secondary data were obtained from the design drawings and specifications of the pile foundation, as well as the manufacturer's certified load capacity for the foundation piles.

This study focuses on a comparative analysis of the bearing capacity of the piles as determined by various methods developed for both design and evaluation of implementation results during construction. The dependent variable in this study is the bearing capacity of the foundation piles for Building F2, while the independent variables include corrected *NSPT* values, *CPT* values, and capacity calculations using several formulas, including *Meyerhof*, *Poulos & Davis*, *Schmertmann*, *Coyle & Castillo*, as well as the Alpha and Lambda Methods. Additionally, dynamic calculations using the *Hiley* formula and *ENR* modification, as well as static load testing with the *Chin* and *Mazurkiewicz* methods, are considered.

The bearing capacity of the pile foundation is defined as the ability of the pile to support the load of the superstructure, while the corrected *NSPT* value refers to adjustments made to the SPT results obtained during the soil investigation to account for field conditions. By collecting *NSPT*, *CPT*, pile driving records, and static and dynamic load testing data, this study aims to comprehensively evaluate the bearing capacity of foundation piles and provide relevant recommendations for future construction projects.

RESULTS AND DISCUSSION

A. Soil Stratification Based on Soil Research Samples and NSPT Values.

Based on the data obtained, the results of the soil layer reading from the soil investigation report can be seen in the following table.

BH-12		BH-15		BH-17	
Jenis	Konsistensi	Jenis	Konsistensi	Jenis	Konsistensi
Lempung kelanauan	Stiff	Lempung kelanauan	Stiff	Lempung kelanauan	Stiff
Lempung kelanauan	Stiff	Lempung kelanauan	Stiff	Lempung kelanauan	Stiff
Lempung kelanauan	Stiff	Lempung kelanauan	Stiff	Lempung kelanauan	Stiff
Lempung kelanauan	Stiff	Lempung kelanauan	Stiff	Lempung kelanauan	Stiff
Lempung kelanauan	Stiff	Lempung kelanauan	Stiff	Lempung kelanauan	Stiff
Lanau kelempungan	Very stiff	Lanau	Very stiff	Lanau	Very stiff
Lanau kelempungan	Very stiff	Lanau	Very stiff	Lanau	Very stiff
Lempung kelanauan	Stiff to very stiff	Lempung kelanauan	Stiff	Lanau	Very stiff
Lempung kelanauan	Stiff to very stiff	Lempung kelanauan	Stiff	Lanau	Very stiff
Lempung kelanauan	Stiff to very stiff	Lempung kelanauan	Stiff	Lanau	Hard
Lempung kelanauan	Stiff to very stiff	Lempung kelanauan	Stiff	Lanau	Hard
Lempung kelanauan	Stiff to very stiff	Lanau	Stiff to hard	Lanau	Hard
Lempung kelanauan	Stiff to very stiff	Lanau	Stiff to hard	Lanau	Hard
Lanau Berbatu	Hard	Lanau	Stiff to hard	Lanau	Hard
Lanau Berbatu	Hard	Lanau	Stiff to hard	Lanau	Hard
Lanau Berbatu	Hard	Lanau sisipan gravel	Hard	Lanau sisipan gravel	Very hard
Lanau Berbatu	Hard	Lanau sisipan gravel	Hard	Lanau sisipan gravel	Very hard
Lanau	Hard	Lanau	Hard	Lanau sisipan gravel	Very hard
Lanau	Hard	Lanau	Hard	Lanau sisipan gravel	Very hard
Lanau	Hard	Lanau	Hard	Lanau sisipan gravel	Very hard
Lanau	Hard	Lanau	Hard	Lanau sisipan gravel	Very hard
Lanau	Hard	Lanau sisipan gravel	Very hard	Lanau sisipan gravel	Very hard
Lanau	Hard	Lanau sisipan gravel	Very hard	Lanau sisipan gravel	Very hard
Lanau Membatu	Very hard	Lanau Membatu	Very hard	Lanau Membatu	Very hard
Lanau Membatu	Very hard	Lanau Membatu	Very hard	Lanau Membatu	Very hard
Lanau Berbatu	Very hard	Lanau Membatu	Very hard	Lanau sisipan gravel	Very hard
Lanau Berbatu	Very hard	Lanau Membatu	Very hard	Lanau sisipan gravel	Very hard
Lanau Membatu	Very hard	Lanau Membatu	Very hard	Lanau sisipan gravel	Very hard
Lanau Membatu	Very hard	Lanau Membatu	Very hard	Lanau sisipan gravel	Very hard
Lanau Membatu	Very hard	Lanau Kepasiran	Hard	Lanau sisipan gravel	Very hard
Lanau Membatu	Very hard	Lanau Kepasiran	Hard	Lanau sisipan gravel	Very hard

Figure 1. Table of Soil Layer Readings from Soil Survey Reports

Source: Primary Data, 2024 (appendix 5)

The table below is a table of soil stratification from the value of N-SPT.

Soil	Layer						
	BH-12			BH-15			BH-17
Lempung kelanauan Stiff	4	4	4	4	4	4	4
Lanau kelempungan Very stiff	2	2	0	0	0	0	0
Lanau Very stiff	0	0	2	2	2	4	4
Lempung kelanauan Stiff to very stiff	6	6	0	0	0	0	0
Lempung kelanauan Stiff	0	0	4	4	4	0	0
Lanau Berbatu Hard	4	4	0	0	0	0	0
Lanau Stiff to hard	0	0	4	4	4	0	0
Lanau sisipan gravel Hard	0	0	2	2	2	0	0
Lanau Hard	6	6	4	4	4	6	6
Lanau sisipan gravel Very hard 1	0	0	2	2	2	8	8
Lanau Membatu Very hard 1	2	2	3	3	3	2	2
Lanau Berbatu Very hard	2	2	0	0	0	0	0
Lanau Membatu Very hard 2	4	4	3	3	3	0	0
Lanau Kepasiran Hard	0	0	2	2	2	0	0
Lanau sisipan gravel Very hard 2	0	0	0	0	0	6	6

Figure 2. Table of Soil Stratification of N-SPT Value

Source: Primary Data, 2024 (appendix 5)

Meanwhile, the value of N-SPT weighing in the field can be seen in the following table.

N-SPT			
Depth (m)	BH-12	BH-15	BH-17
0	0	0	0
2	14	12	13
4	12	10	15
6	17	20	17
8	15	11	23
10	14	13	32
12	21	15	30
14	36	48	45
16	41	48	60
18	46	52	60
20	41	48	60
22	48	60	60
24	60	60	60
26	60	60	60
28	60	60	60
30	60	51	60

Figure 3. Table of N-SPT Field Reading Scores
Source: Primary Data, 2024 (appendix 5)

SOIL PARAMETER	TESTING	SYMBOL	BH-12			BH-15			BH-17		
			1.50-2.00	3.50–4.00	5,50–6.00	1.50-2.00	3.50–4.00	5,50–6.00	1.50-2.00	3.50–6.00	5,50–6.00
INDEX PROPERTIES	WATER CONTENT	W (%)	50	67	58	47,28	69,52	62,02	47	54	50
	UNIT WEIGHT	γ (ton/m³)	1,54	1,38	1,46	1,63	1,45	1,49	1,63	1,6	1,65
	VOID RATIO	e	1,67	2,27	1,96	1,38	2,02	1,85	1,45	1,63	1,51
	SPECIFIC GRAFITY	Gs	2,73	2,71	2,72	2,64	2,59	2,61	2,71	2,73	2,76
	DEGREE OF SATURATION	Sr (%)	82,32	80,04	81,05	90,38	89,19	87,77	87,96	90,48	91,66
	ATTERBERG	LL (%)	103,21	103,15	94,9	93,92	92,31	90,64	102,46	102,05	98,42
		PI (%)	49,23	55,31	52,06	44,83	51,88	49,27	57,2	55,58	56,51
	GRAND SIZE DISTRIBUTIONS	Gravel (%)	0	0	0	0	0	0	0	0	0
		Sand (%)	4,95	4,98	1,8	5,5	4,83	6,48	6,77	4,76	11,25
		Silt (%)	21,02	17,88	25,71	77,5	67,87	55,82	22,53	37,36	42,27
		Clay (%)	74,03	77,14	72,49	17	27,2	37,7	70,7	57,86	46,48
GINEERING PROPERT	TRIAXIAL UU	C (kg/cm2)	0,38	0,36	0,32	0,32	0,3	0,24	0,48	0,46	0,43
		ϕ (°)	7	7	5	19,48	16,09	15,83	6	6	6
	CONSOLIDATION	Cc	0,26	0,46	0,47	0,22	0,18	0,13	0,24	0,4	0,48
		Pc (kg/cm2)	2,14	2,24	2,12	2,8	2,8	2,88	2,4	2,42	2,1
		Cv (cm2/sec)	0,00014	0,00014	0,00014	0,00808	0,00842	0,00842	0,00015	0,00014	0,00014

Figure 4. Table of Soil Parameters
Source: Primary Data, 2024 (appendix 7)

Correction of NSPT values based on Skemton and Terzaghi.

The corrected N-SPT value according to Skemton can be seen in the following table:

N60 (Skempton, 1986)			
Depth (m)	BH-12	BH-15	BH-17
0	0,000	0,000	0,000
2	12,775	10,950	11,863
4	10,950	9,125	13,688
6	15,513	18,250	15,513
8	13,688	10,038	20,988
10	12,775	11,863	29,200
12	19,163	13,688	27,375
14	32,850	43,800	41,063
16	37,413	43,800	54,750
18	41,975	47,450	54,750
20	37,413	43,800	54,750
22	43,800	54,750	54,750
24	54,750	54,750	54,750
26	54,750	54,750	54,750
28	54,750	54,750	54,750
30	54,750	46,538	54,750

Figure 5. Table of N-SPT Value Table Corrected According to Skemton

Source: Primary Data, 2024 (appendix 5)

Based on the N-SPT value and the corrected N-SPT value according to Skemton, a soil stratification graph was made as seen in the graph below:

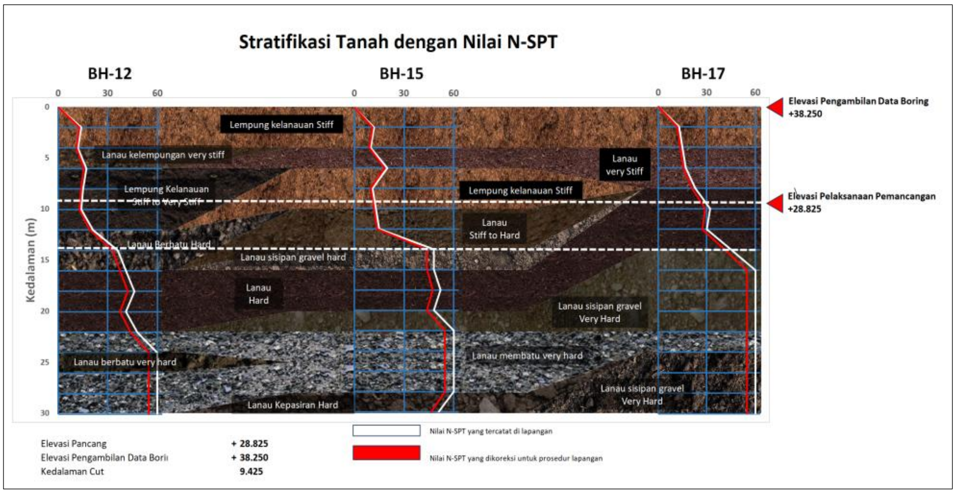

Figure 6. Soil Stratification Drawing, N-SPT Value and N-SPT Value corrected according to Skemton

The corrected N-SPT value according to Terzaghi can be seen in the following table:

N60 (Terzaghi)			
Depth (m)	BH-12	BH-15	BH-17
0	0,000	0,000	0,000
2	14,000	12,000	13,000
4	12,000	10,000	15,000
6	15,513	18,250	15,513
8	15,000	11,000	20,988
10	14,000	13,000	29,200
12	19,163	15,000	27,375
14	32,850	43,800	41,063
16	37,413	43,800	54,750
18	41,975	47,450	54,750
20	37,413	43,800	54,750
22	43,800	54,750	54,750
24	54,750	54,750	54,750
26	54,750	54,750	54,750
28	54,750	54,750	54,750
30	54,750	46,538	54,750

Figure 8. table of N-SPT Value Table Corrected According to Terzaghi
Source: Primary Data, 2024

Based on the N-SPT value and the corrected N-SPT value according to Terzaghi, a soil stratification graph was made as seen in the graph below:

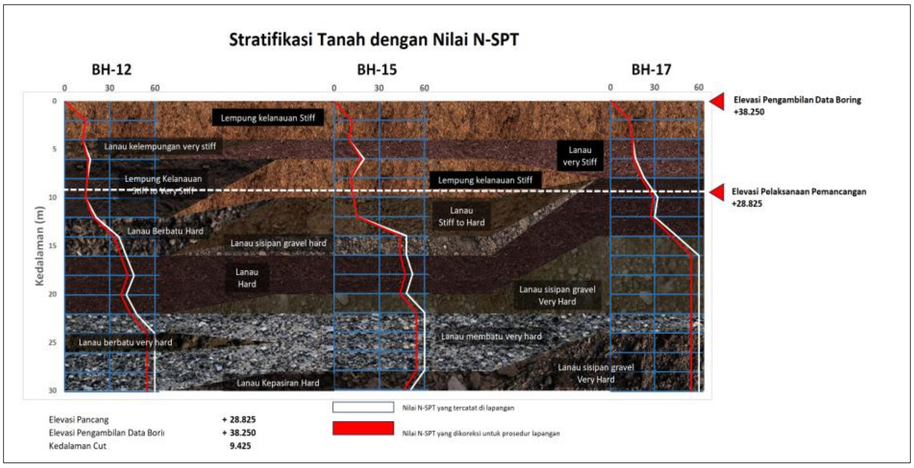

Figure 9. Soil Stratification Drawing, N-SPT Value and N-SPT Value Corrected According to Terzaghi

The calculation of the peak bearing capacity uses the Meyerhoff (1956) formula with the correction of NSPT values based on Terzaghi and Skemton.

Using the Mayerhoff Formula below, Tomlinson, M. J. (2001);

$Q_u=40*N_b*A_p +0.2*\bar{N}*A_s$ .... (22)

…… For Clay Soil the coefficient of 0.2 is changed to 0.5

N_b = Average NSPT value at depth near the tip of the pole (toe) or zone of influence of the tip

A_p = Cross-sectional area of the end of the pole (m²)

$\bar{N}$ = Average NSPT value along the pole rod in the ground shear zone

A_s = Side surface area of the pole (m²)

Hence the Qu NSPT Skemton correction and Terzaghi correction for Drill Hole (BH) 12, 15 and 17 are as follows:

Tabel 1. Qu NSPT Skemton correction and Terzaghi

No	*Location*	**Qu NSPT Correction Skempton**				**Qu NSPT Terzaghi Correction**			
1.	BH - 12	Nb	=	54,75		Nb	=	54,75	
		Ap	=	0,0625	m²	Ap	=	0,0625	m²
		$\bar{N}$	=	37,35167		$\bar{N}$	=	37,515	
		As	=	24	m²	As	=	24	m²
		That	=	585,095	kn	That	=	587,055	kn
			=	59,66331	Tone		=	59,86317	Tone
2.	BH - 15	Nb	=	54,75		Nb	=	54,75	
		Ap	=	0,0625	m²	Ap	=	0,0625	m²
		$\bar{N}$	=	39,86923		$\bar{N}$	=	40,24615	
		As	=	24	m²	As	=	24	m²
		That	=	615,3058	kn	That	=	619,8288	kn
			=	62,74396	Tone		=	63,20519	Tone
3.	BH - 17	Nb	=	54,75		Nb	=	54,75	
		Ap	=	0,0625	m²	Ap	=	0,0625	m²
		$\bar{N}$	=	43,53929		$\bar{N}$	=	43,53929	
		As	=	24	m²	As	=	24	m²
		That	=	659,3464	kn	That	=	659,3464	kn
			=	67,23487	Tone		=	67,23487	Tone

Source : Primary Data, 2024

Based on the results of the calculation above, the results of the Qu pile foundation pile rounded into two numbers behind the comma can be seen in the following table.

Table 2. The Table of Values Qu of Meyerhoff's Formula (1956) is corrected according to Skemton and Terzaghi

Qu Pile Foundation Pile	**BH-12 Tone**	**BH-15 Tone**	**BH-17 Tone**
Qu Meyerhoff (1956) NSPT Skemton Correction	59,66	62,74	67,23
Qu Meyerhoff (1956) NSPT Koreksi Terzaghi	59,86	63,21	67,23

Source: Primary Data, 2024 (appendix 5)

Calculation of peak carrying capacity using the Poulus & Davis formula

Calculation using BH12, L Pole =15m:

Qu=∑...(β β σ ^'_(rata-rata)=A_s)+(c=Nc)=A_b .... (23)

Qu=∑▒〖(0.25·(1.46 tons/m^3·15 m)/2·0.25 m·4·15 m)〗+(3.2 tons/m^2·9)·0.25 m·0.25 m

Qu=41.0625 ton+1.8 ton

Qu=42.8625 tons

Calculation using BH15, L Pole =13m:

Qu=∑...(β β σ ^'_(rata-rata)=A_s)+(c=Nc)=A_b .... (24)

Qu=∑▒ 〖(0.25·(1.49 tons/m^3·13 m)/2·0.25 m·4·13 m)〗 +(2.4 tons/m^2·9)·0.25 m·0.25 m

Qu=31.4763 ton+1.35 ton

Qu=32.8263 ton

Calculation using BH17 , L Pole =12m:

Qu=∑...(β β σ ^'_(rata-rata)=A_s)+(c=Nc)=A_b .... (25)

Qu=∑▒ 〖(0.25·(1.65 tons/m^3·12 m)/2·0.25 m·4·12m)〗 +(4.3 tones/m^2·9)·0.25 m·0.25 m

Qu=29.7 ton+2.4188 ton

Qu=32.1188 tons

Calculation of peak bearing capacity using the Schmrecment formula

Based on the primary data collection at the research location, the sondir value was obtained as seen in the following table:

Titik Sondir	Kedalaman Penyondiran (m)	Kedalaman Pada qc ≥ 100 kg/cm2 (m)	Nilai tf pada Nilai qc ≥ 100 kg/cm2 (kg/cm)	Nilai qc pada Kedalaman 1,00 m (kg/cm^2)	Nilai qc pada Kedalaman 2,00 m (kg/cm^2)
S9	12	11	760	15	14
S12	8	7,4	380	20	20
S15	11,6	10,4	640	25	16

Figure 10. Table of Sondir's Value

Source: Primary Data, 2024 (Appendix 5)

Calculation using S9 equifalen BH12,

α=0.4 for wetlands and Nc=0.5 for wetlands

Qu= ∑...(α .tf+K)+Nc.qc.A_(b) * .... (26)

Qu= ∑▒ 〖(0.4 .7.6 tons/m·0.25m·4)+0.5.(1000 tons/m2).0.25m·0.25m〗

Qu= 3.04 ton+31.25 ton

Qu= 34.29 Tons

Calculation using S12 equifalen BH15,

α=0.4 for wetlands and Nc=0.5 for wetlands

Qu= ∑...(α .tf+K)+Nc.qc.A_(b) * .... (27)

Qu= ∑▒ 〖(0.4 .3.8 tons/m·0.25m·4)+0.5.(1000 tons/m2).0.25m·0.25m〗

Qu= 1.52 ton+31.25 ton

Qu= 32.77 Tons

The calculation uses S15 equifalen BH17, α=0.4 for silt soil and Nc=0.5 for silt soil

Qu= ∑??(α .tf+K)+Nc.qc.A_(b) ....It's not. (28)

Qu= ∑▒〖(0.4 .6.4 tons/m·0.25m·4)+0.5.(1000 tons/m2).0.25m·0.25m〗

Qu= 2.56 ton+31.25 ton

Qu= 33.81 Tons

Calculation of peak carrying capacity using the Coyle & Castilo formula

Calculation using S9 equifalen BH12,

α=0.4 for silt and Kb=0.7 for silt

Qu= ∑...(α .tf+K)+Kb.qc.A_(b) .... (29)

Qu= ∑▒〖(0.4 .7.6 tons/m·0.25m·4)+0.7.(1000 tons/m2).0.25m·0.25m〗

Qu= 3.04 ton+43.75 ton tone

Qu= 46.79 Tons

Calculation using S12 equifalen BH15,

α =0.4 for silt and Kb=0.7 for silt

Qu= ∑...(α .tf+K)+Kb.qc.A_(b) .... (30)

Qu= ∑▒〖(0.4 .3.8 tons/m·0.25m·4)+0.7.(1000 tons/m2).0.25m·0.25m〗

Qu= 1.52 ton+43.75 ton

Qu= 45.27 Ton

Calculation using S15 equifalen BH17,

α =0.4 for silt and Kb=0.7 for silt

Qu= ∑...(α .tf+K)+Kb.qc.A_(b) .... (31)

Qu= ∑▒〖(0.4 .3.8 tons/m·0.25m·4)+07.(1000 tons/m2).0.25m·0.25m〗

Qu= 2.56 ton+43.75 ton

Qu= 46.31 Tons

Calculation of peak bearing capacity using the formula of the Alpha & Lamda Method

Calculation using S9 equifalen BH12,

α =0.4 for silt land and,

Nc=9 Based on Terzaghi and Meyerhof

Qu= ∑▒〖(α . Cu·A_(s))+Nc×cu×At〗 .... (32)

Qu= ∑▒〖(0.4 .3.2 tons/m2·0.25m·4·15m)+9.(3.2 tons/m2).0.25m·0.25m〗

Qu= 19.2 ton+1.8 ton

Qu= 21.00 Ton

Calculation using S12 equifalen BH15,

α =0.4 for silt land and,

Nc=9 Based on Terzaghi and Meyerhof

Qu= ∑▒〖(α . Cu·A_(s))+Nc×cu×At〗 ……………………………… (33)

$Qu = \sum [(0.4 \,.\, 2.4 \text{ tons/m2} \cdot 0.25\text{m} \cdot 4 \cdot 13\text{m}) + 9.(2.4 \text{ tons/m2}).0.25\text{m} \cdot 0.25\text{m}]$

Qu= 12.48 ton+1.35 ton

Qu= 13.83 Tons

Calculation using S15 equivalent BH17,

α =0.4 for silt land and,

Nc=9 Based on Terzaghi and Meyerhof

$Qu = \sum [(\alpha \,.\, Cu \cdot A_{(s)}) + Nc \times cu \times At]$ .... (34)

$Qu = \sum [(0.4 \,.\, 4.3 \text{ tons/m2} \cdot 0.25\text{m} \cdot 4 \cdot 12\text{m}) + 9.(4.3 \text{ tons/m2}).0.25\text{m} \cdot 0.25\text{m}]$

Qu= 20.64 ton+2.42 ton

Qu= 23.06 Tons

Calculation of peak bearing capacity using the Hiley Dynamic formula

The Single Pole Capacity data based on the Hiley Formula can be seen in appendix 1 with the average result as shown in the table below.

Table 3. Single Pole Capacity based on the Hiley Formula

	Average Score
Qu (Tone)	294,57
Qu Izin (Ton)	147,28

Source: Primary Data, 2024 (Appendix 9)

Based on the data from the table above, the carrying capacity of the peak pile based on the Hiley formula is 294.57 tons.

1. Calculation of peak bearing capacity using the ENR Modified Dynamic formula

The Single Pole Capacity data based on the Modified ENR Formula can be seen in appendix 2 with average results as shown in the table below.

Table 4. Single Pole Capacity based on ENR Modification

	Average Score
Qu (Tone)	271,10
Qu Izin (Ton)	108,43

Source: Primary Data, 2024 (Appendix 10)

Based on the data from the table above, the carrying capacity of the peak pile based on the ENR modified dynamic formula is 271.10 tons.

2. Static test load analysis using Mazurkiewich and Chin methods

The results of the foundation pole test on axial pressure loading of axial unused axial #1 to axial #1 can be seen in appendix 11. From the data of the test results, the ultimate load interpretation curve was obtained using the Mazurkiewich method (Figure IV-3) and the ultimate load interpretation curve with the Chin method (Figure IV-4).

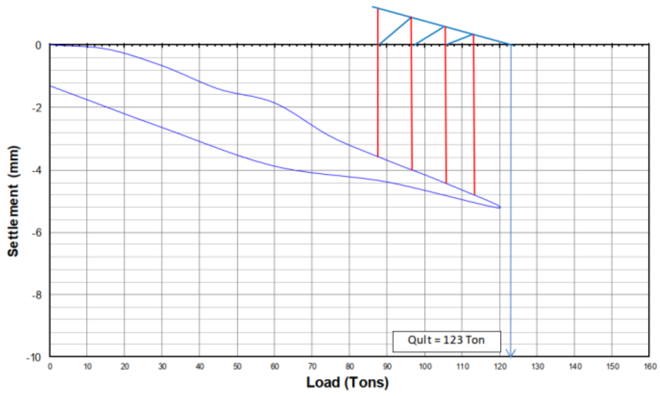

Unused Axial #1(F2)

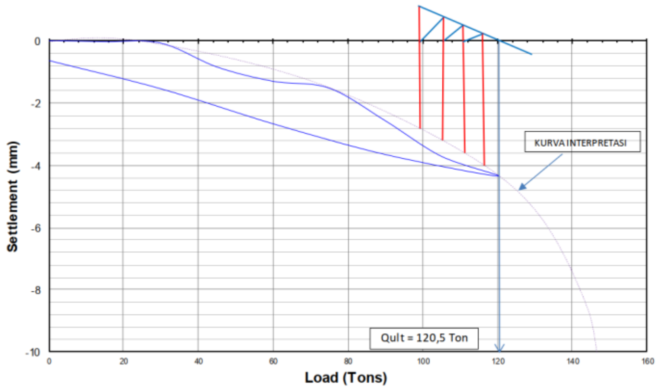

Unused Axial #2(F2)

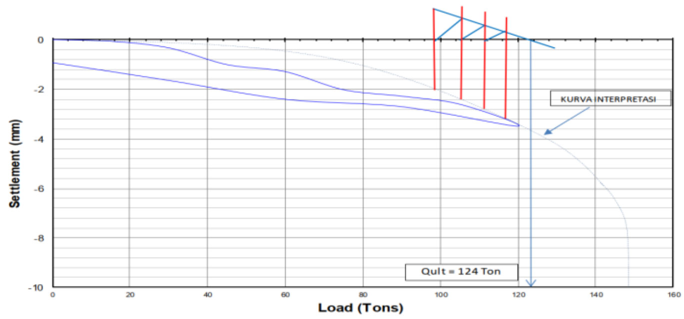

Unused Axial #3(F2)

Figure 11. Mazurkiewich Method Ultimate Load Interpretation Curve
Source : Project X Static Testing Report, 2023

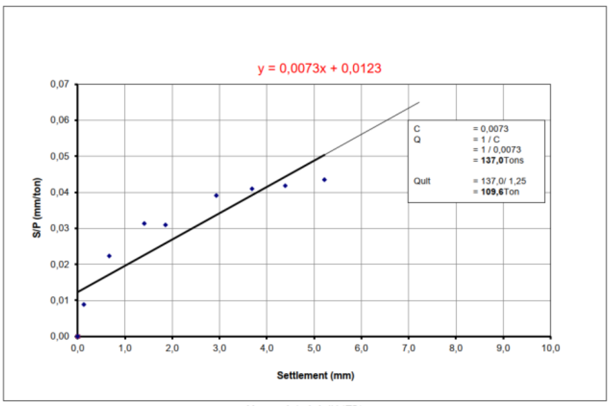

Unused Axial #1(F2)

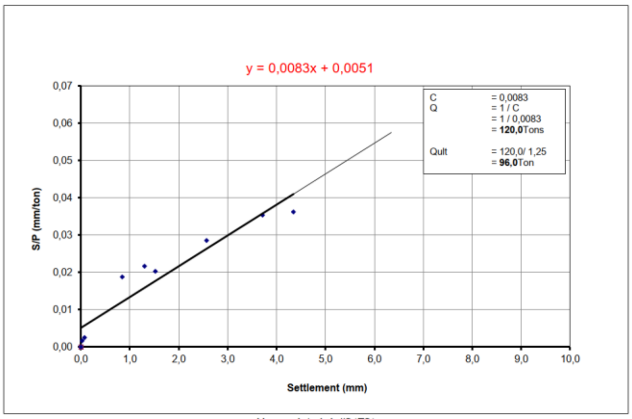

Unused Axial #2(F2)

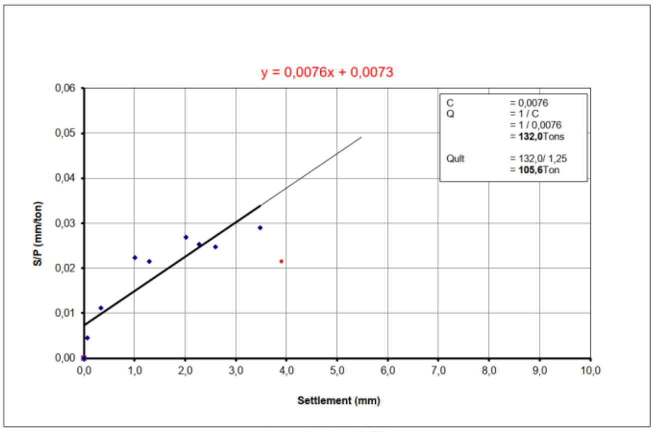

Unused Axial #3(F2)

Figure 12. Chin Method Ultimate Load Interpretation Curve
Source : Project X Static Testing Report, 2023

3. Dynamic test load analysis using CAPWAP

The Bearing Capacity of the Pole Based on the CAPWAP Results can be seen in the following table.

Nomor Tiang Uji	Daya dukung tiang [ton]				BTA (%)
	PDA (ton)	CAPWAP Total (ton)	CAPWAP Lekatan (ton)	CAPWAP Tahanan ujung (ton)	
P-238-18B	113	124.1	41.0	83.2	100
P-492-2B	189	197.5	60.0	137.5	100

Table 13. Pole Bearing Capacity Based on CAPWAP Results

Source: Primary Data, 2024 (the results of the CAPWAP reading are in Appendix 12).

4. Validation of the Peak Bearing Capacity of the Foundation of the Static Formula Meyerhoff (1956) NSPT Correction of Terzaghi and Skemton, Poulus & Davis, Schmrecment, Coyle & Castilo, and the Alpha & Lamda Method with Static (Mazurkiewich & Chin) and Dynamic (CAPWAP) Test Results

The Qu value of the calculation using the Static formula of Meyerhoff (1956) NSPT Terzaghi and Skemton, Poulus & Davis, Schmrecment, Coyle & Castilo, as well as the Alpha & Lamda Method and the Static (Mazurkiewich & Chin) and Dynamic (CAPWAP) Test Results can be seen in the graph below

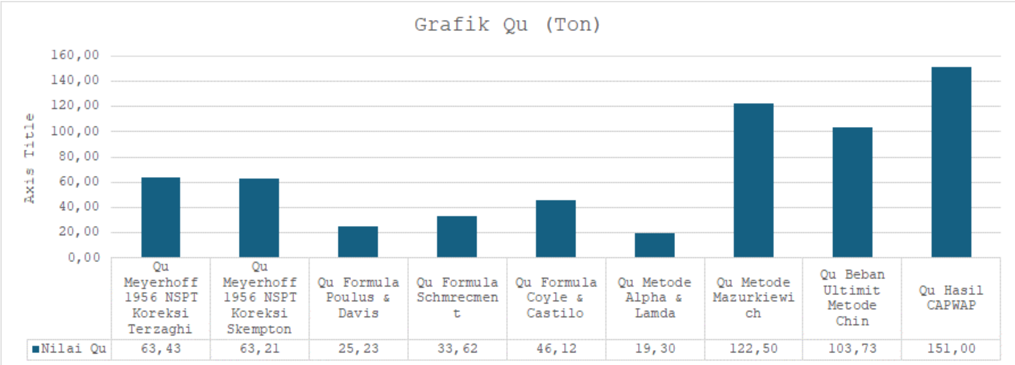

Figure 14. Qu values from the calculation using the Static formula Meyerhoff (1956) NSPT Terzaghi and Skemton, Poulus & Davis, Schmrecment, Coyle & Castilo, as well as the Alpha & Lamda Method and the Static (Mazurkiewich & Chin) and Dynamic (CAPWAP) Test Results

Based on the Qu value in the graph above, the validation results between the Static Meyerhoff (1956) NSPT Terzaghi and Skemton Corrections, Poulus & Davis, Schmrecment, Coyle & Castilo, as well as the Alpha & Lamda Method and the Static (Mazurkiewich & Chin) and Dynamic (CAPWAP) Test Results can be seen in this table

Table 5. Percentage Value Deviation to Qu validator

Qu Validator	Percentage Value Deviation to Qu validator					
	Qu Meyerhoff 1956 NSPT Koreksi Terzaghi	Qu Meyerhoff 1956 NSPT Correction Skemton	Qu Formula Poulus & Davis	Qu Formula Schmrecment	Qu Formula Coyle & Castilo	Qu Alpha & Lamda Method
Qu Metode Mazurkiewich	51,78%	51,60%	20,60%	27,45%	37,65%	15,75%
Qu Ultimate Load Chin Method	61,15%	60,94%	24,32%	32,41%	44,46%	18,60%
Qu CAPWAP Results	42,01%	42,01%	16,71%	22,27%	30,55%	12,78%

Source: Primary Data, 2024 (appendices 5 & 7)

Based on the percentages of the table above, the results of the peak bearing capacity that are closest to the static and dynamic test results are Qu Mayerhoff 1956 NSPT Terzaghi correction.

5. Validation of the results of the calculation of peak bearing capacity based on calculations with Hiley formulas and modified ENR with Static (Mazurkiewich & Chin) and Dynamic (CAPWAP) Test Results

The Qu value of the calculation results using the Hiley dynamic formula and modified ENR and the Static (Mazurkiewich & Chin) and Dynamic Test Results (CAPWAP) can be seen in the graph below

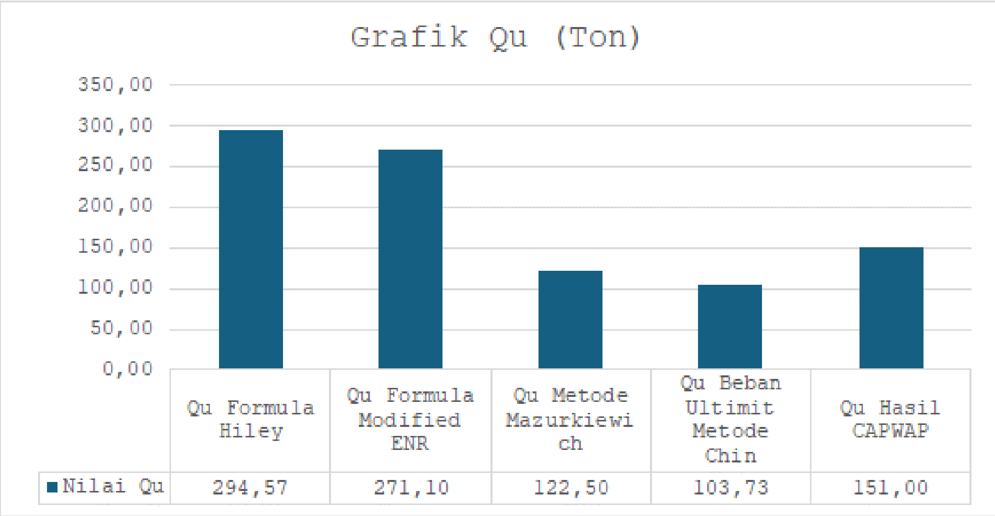

Figure 15. Qu values of the calculation results using the modified Hiley and ENR dynamic formulas and Static (Mazurkiewich & Chin) and Dynamic (CAPWAP) Test Results

Based on the Qu value in the graph above, the validation results between the Hiley dynamic formula and the modified ENR and the Static (Mazurkiewich & Chin) and Dynamic (CAPWAP) Test Results can be seen in this table

Qu Validator	Prosentase Nilai Deviasi terhadap Qu validator	
	Qu Formula Hiley	Qu Formula Modified ENR
Qu Metode Mazurkiewich	240,47%	221,31%
Qu Beban Ultimit Metode Chin	283,97%	261,34%
Qu Hasil CAPWAP	195,08%	179,54%

Figure 16. Percentage Value Deviation to Qu validator

Based on the percentage of the table above, the results of the peak carrying capacity that are closest to the static and dynamic test results are the ENR Modified Qu Formula.

6. Comparison of results Validate peak bearing capacity with allowable loads from designs and allowable loads from manufacturing.

The validation result of the static formula was Qu Mayerhoff 1956 NSPT Terzaghi correction, while for the dynamic formula Qu Formula Modified ENR and compared with the design carrying capacity and carrying capacity of the manufacturing permit by eliminating the Mayerhoff 1956 static calculation.

Based on the results of the comparison, there is a difference that can be more efficient from the selected pole with a manufacturing capacity of 80 Tons to the need for a 200% design carrying capacity of 70 tons, as seen in the graph below.

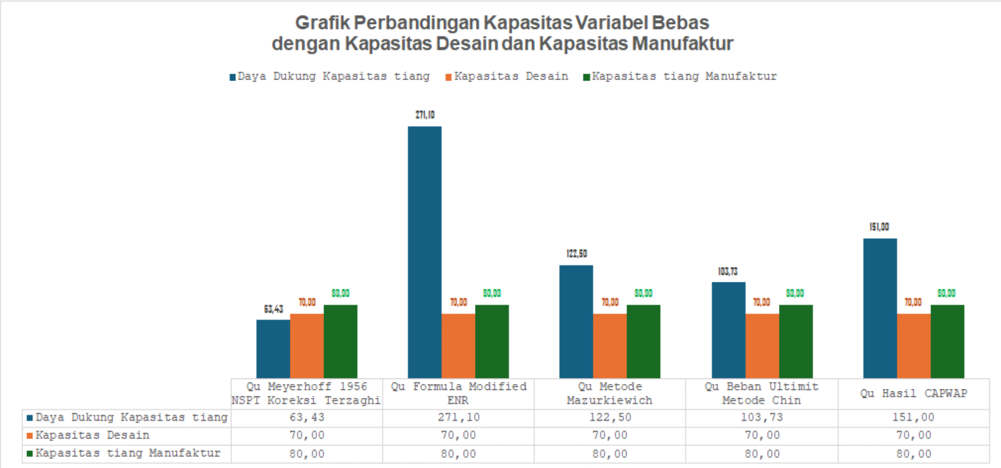

Figure 17. Comparison Chart of Free Variable Capacity with Design Capacity and Manufacturing Capacity

CONCLUSION

Based on the comparison graph of pile bearing capacities using various formulas and methods against the design and manufacturing capacities, it was found that the Mazurkiewich Method, Chin Method, and CAPWAP analysis yielded bearing capacity values higher than both the design capacity (35 tons, with an ultimate capacity of 70 tons at a 200% safety factor) and the manufacturing capacity. This indicates that the selected pile type can still be optimized for greater efficiency. Static and dynamic tests served as validators, and the most valid calculation results were those closest to these validator values. Specifically, the Meyerhoff 1956 method with NSPT Terzaghi Correction produced results most consistent with static and dynamic tests, followed by the Meyerhoff 1956 NSPT Skempton Correction, Coyle & Castillo, Schmertmann, Poulos & Davis, and Alpha and Lambda Methods, with the latter providing the lowest ultimate capacity. For dynamic formulas, the Modified ENR formula gave results closest to dynamic test values, while among static methods, the Mazurkiewich Method most closely matched CAPWAP dynamic test results. For future research, it is recommended to explore the application of advanced numerical modeling and real-time monitoring technologies to further refine the accuracy and efficiency of pile foundation design and assessment in manufacturing construction projects.

REFERENCES

Awad, T., Guardiola, J., & Fraíz, D. (2021). Sustainable construction: Improving productivity through lean construction. *Sustainability (Switzerland)*, *13*(24). https://doi.org/10.3390/su132413877

Belaroussi, R., Dai, H., González, E. D., & Gutiérrez, J. M. (2023). Designing a Large-Scale Immersive Visit in Architecture, Engineering, and Construction. *Applied Sciences (Switzerland)*, *13*(5). https://doi.org/10.3390/app13053044

Chen, D., Zhou, J., Duan, P., & Zhang, J. (2023). Integrating knowledge management and BIM for safety risk identification of deep foundation pit construction. *Engineering, Construction and Architectural Management*, *30*(8). https://doi.org/10.1108/ECAM-10-2021-0934

Flynn, K. N., & McCabe, B. A. (2019). Driven cast-in-situ piles installed using hydraulic hammers: Installation energy transfer and driveability assessment. *Soils and Foundations*, *59*(6). https://doi.org/10.1016/j.sandf.2019.09.003

GENDRON GJ. (1970). PILE DRIVING. HAMMERS AND DRIVING METHODS. *Highw Res Rec*, *33*.

Gernsbacher, M. A. (1991). Cognitive Processes and Mechanisms in Language Comprehension: The Structure Building Framework. *Psychology of Learning and Motivation - Advances in Research and Theory*, *27*(C). https://doi.org/10.1016/S0079-7421(08)60125-5

Khosravani, M. R., & Haghighi, A. (2022). Large-Scale Automated Additive Construction: Overview, Robotic Solutions, Sustainability, and Future Prospect. *Sustainability (Switzerland)*, *14*(15). https://doi.org/10.3390/su14159782

Liu, Z., Ng, A. H. M., Wang, H., Chen, J., Du, Z., & Ge, L. (2023). Land subsidence modeling and assessment in the West Pearl River Delta from combined InSAR time series, land use and geological data. *International Journal of Applied Earth Observation and Geoinformation*, *118*. https://doi.org/10.1016/j.jag.2023.103228

Mechtcherine, V., Nerella, V. N., Will, F., Näther, M., Otto, J., & Krause, M. (2019). Large-scale digital concrete construction – CONPrint3D concept for on-site, monolithic 3D-printing. *Automation in Construction*, *107*. https://doi.org/10.1016/j.autcon.2019.102933

Nietiedt, J. A., Randolph, M. F., Gaudin, C., & Doherty, J. P. (2023). Development of a high-energy centrifuge model impact hammer for pile-driving. *International Journal of Physical Modelling in Geotechnics*, *24*(2). https://doi.org/10.1680/jphmg.21.00096

Puzatova, A., Shakor, P., Laghi, V., & Dmitrieva, M. (2022). Large-Scale 3D Printing for Construction Application by Means of Robotic Arm and Gantry 3D Printer: A Review. In *Buildings* (Vol. 12, Issue 11). https://doi.org/10.3390/buildings12112023

Saher, H. S., Al-Jubair, H. S., & Ali, J. K. (2024). Measurements of induced vibrations due to steel pipe pile driving in Al-Fao soil: Effect of partial end closure. *Open Engineering*, *14*(1). https://doi.org/10.1515/eng-2022-0550

Svatoš-Ražnjević, H., Orozco, L., & Menges, A. (2022). Advanced Timber Construction Industry: A Review of 350 Multi-Storey Timber Projects from 2000-2021. *Buildings*, *12*(4). https://doi.org/10.3390/buildings12040404

Tang, X., Xu, S., Gong, X., Gu, C., Gong, Y., & Cui, L. (2024). Geological Stratification of Soil Engineering and Its Applications to Urban Underground Space Development. *Geology and Exploration*, *60*(1). https://doi.org/10.12134/j.dzykt.2024.01.018

Zhang, D. M., Jiang, Q. H., Zhang, J. Z., & Huang, H. W. (2024). Bearing capacity of shallow foundations considering geological uncertainty and soil spatial variability. *Acta Geotechnica*, *19*(6). https://doi.org/10.1007/s11440-023-02091-0

Zhao, X. (2024). Construction risk management research: intellectual structure and emerging themes. *International Journal of Construction Management*, *24*(5). https://doi.org/10.1080/15623599.2023.2167303